

MASONRY INFILL WALLS: AN EFFECTIVE ALTERNATIVE FOR SEISMIC STRENGTHENING OF LOW-RISE REINFORCED CONCRETE BUILDING STRUCTURES

Santiago Pujol¹, Amadeo Benavent-Climent², Mario E Rodriguez³, and J. Paul Smith-Pardo⁴

¹ School of Civil Engineering, Purdue University, W. Lafayette, IN, USA

² Department of Structural Mechanics, University of Granada, Granada, Spain

³ Instituto de Ingeniería, UNAM, Mexico City, Mexico

⁴ Berger/Abam Engineers, Inc., Federal Way, WA, USA

ABSTRACT

Masonry infill walls are widely used as partitions worldwide. Field evidence has shown that continuous infill masonry walls can help reduce the vulnerability of a reinforced concrete structure. In order to test this hypothesis, a full-scale three-story flat-plate structure was strengthened with infill brick walls and tested under displacement reversals. The results of this test were compared with results from a previous experiment in which the same building was tested without infill walls. In the initial test, the structure experienced a punching shear failure at a slab-column connection. The addition of infill walls helped to prevent slab collapse and increased the stiffness and strength of the structure. The measured drift capacity of the repaired structure was 1.5 %. A numerical model of the test structure was calibrated to match experimental results. Numerical simulations of the response of the strengthened structure to several scaled ground motion records suggest that the measured drift capacity would not be reached during strong ground motion.

KEYWORDS: Masonry Walls, Infill, Displacement Capacity, Collapse Prevention, Numerical Simulation.

1. INTRODUCTION

RC frames with unreinforced masonry infill walls are common in developing countries with regions of high seismicity. Often, engineers do not consider masonry infill walls in the design process because the final distribution of these elements may be unknown to them, or because masonry walls are regarded as non-structural elements. Separation between masonry walls and frames is often not provided and, as a consequence, walls and frames interact during strong ground motion. This leads to structural response deviating radically from what is expected in the design.

Previous experimental research on the response of RC frames with masonry infill walls subject to static and dynamic lateral cyclic loads (Fiorato et al., 1970; Brokken and Bertero, 1981; Calvi and Bolognini, 2001; Negro and Verzeletti, 1996; Zarnic et al., 2001; Hashemi and Mosalam, 2006) have shown that infill walls lead to significant increases in strength and stiffness in relation to bare RC frames. Within conventional seismic design, which focuses on accelerations and strength, it may be difficult to recognize the benefits of increases in stiffness. However, research and field evidence (Shimazaki and Sozen 1988; Wood, 1991; Lepage, 1997) has shown that increases in stiffness are beneficial because they lead to reductions in the magnitude of the deformations induced by ground motions.

An experimental program was designed to test the hypothesis that masonry walls can be used to reduce the vulnerability of RC frames. The object to the program was to investigate whether the RC-brick composite has enough displacement capacity to sustain displacement cycles in the nonlinear range of response. This question was addressed through an experiment in which a full-scale three-story reinforced-concrete structure that had been

previously tested to failure was tested a second time after strengthening with brick infill walls. This paper describes the results from these tests and their implications.

2. TEST STRUCTURE WITHOUT INFILL WALLS

The original structure was built and tested by Fick (2008). It consisted of a three-story reinforced-concrete structure designed and detailed using U.S. design practices for buildings located in low-seismicity regions. Each floor of the building measured 15 m (50 ft) by 9.1 m (30 ft) in plan (Figure 1). The total height of the structure was 9.15 m (30 ft), each story measuring 3.05 m (10 ft) (from top of slab or footing to top of slab above). Six reinforced concrete columns with 460 mm (18-in.) square cross sections were arranged in two column lines to support three 180-mm (7-in.) thick flat slabs. Columns were supported by 1.4 m (4.5 ft) x 1.4 m (4.5 ft) x 0.76 m (2.5 ft) monolithic footings fastened to the strong floor of Purdue University's Bowen Laboratory using four post-tensioning rods per footing. The compressive strength of concrete cylinders tested at 28 days after casting was 28 MPa (4 ksi). The slabs were reinforced with #4 (D12) bars with a measured yield stress of 470 MPa (68 ksi). Columns had 8 #7 longitudinal bars with a yield stress of 460 MPa (66 ksi). Longitudinal bars of columns had 1.5-m (5-ft) lap splices above footings and slabs. Column ties were made using #3 bars with a yield stress of 520 MPa (75ksi), and were spaced at 220 mm (7 in.) (or $d/2$, with d = effective depth). All reinforcement conformed to ASTM A615.

The structure was loaded with 0.57 kN/m^2 (12 psf) of superimposed dead load using water-filled barrels placed on the slabs before lateral loads were applied.

The initial fundamental period of the structure, estimated from free-vibration tests, was approximately 0.5 sec.

Cyclic lateral loads were applied using six hydraulic actuators; two at each floor. The actuators attached to the top slab were operated through displacement control. Loads applied to the floor of the third story were adjusted to 2/3 of the load at the top level, and the load applied to the floor of the second story was adjusted to and 1/3 of the load at the top level. Four displacement cycles were applied to the original structure with maximum roof drift ratios of ± 0.22 , ± 0.45 , ± 1.5 and $\pm 3.0\%$.

The maximum base shear measured was approximately one third of the weight of the structure (including superimposed loads). The test was stopped after the first complete cycle at 3.0%. When the roof drift ratio reached 2.8% in the second half of this cycle, a punching shear failure took place (Fick, 2008).

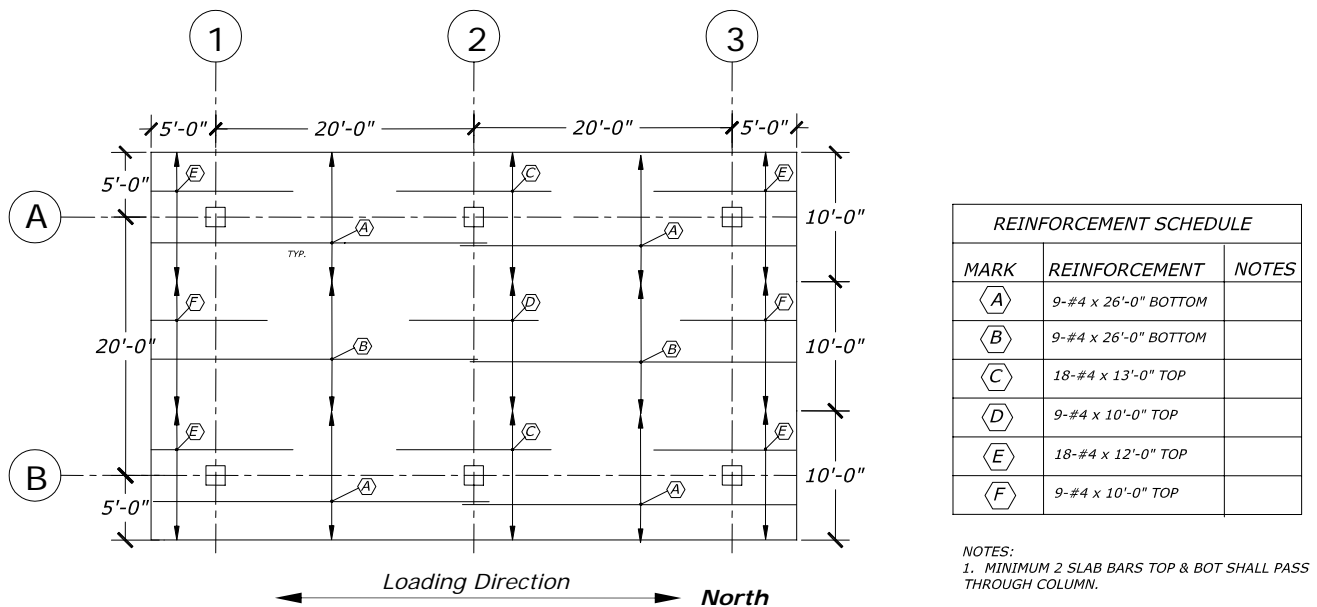


Figure 1. Plan View of Test Structure.

3. STRENGTHENING OF THE TEST STRUCTURE WITH INFILL WALLS

In each story, two full-height continuous unreinforced brick walls were built in the direction of loading as shown in Figure 2. The ratio of the cross-sectional area of walls to the total floor area of the test structure was:

$$\frac{\text{nominal wall thickness} \times \text{center-to-center bay length} \times \text{number of walls}}{\text{number of stories} \times \text{typical floor area}} = \frac{92\text{mm} \times 6.1\text{m} \times 2}{3 \times 9.1\text{m} \times 15.2\text{m}} = 0.27\%$$



Figure 2. Test Structure with Infill Walls

The mortar used to build the infill walls was made with QUIKRETE® Mortar Mix (No. 1102); a blend of masonry cement and graded sand meeting ASTM C 270 for Type N Mortar. Its average compressive strength, obtained from tests of 45 50-mm (2-in.) cubes, was 10 MPa (1500 psi) and the corresponding standard deviation was 2.8 MPa (400 psi). Tests of 29 100x200-mm (4x8-in.) cylinders yielded an average strength of 12 MPa (1700 psi) and a standard deviation of 4.1 MPa (600 psi).

Masonry walls were made of solid clay bricks with a thickness of 92mm (3-5/8 in.), a depth (vertical dimension) of 57mm (2-1/4 in.), and a length of 194mm (7-5/8 in.). Masonry compressive strength, computed on the basis of total gross area and the results of tests of 4-brick prisms subjected to axial load perpendicular to mortar joints, was 38 MPa (5500 psi). The density of the masonry was measured to be 2100 kg/m³ (130pcf).

The strength of the masonry in diagonal compression was evaluated by testing two series of three wall samples each. The nominal dimensions of the samples in Series 1 were 300 x 300 x 92 mm (12 x 12 x 3-5/8 in.). The nominal dimensions of the samples in Series 2 were 250 x 300 x 92 mm (10 x 12 x 3-5/8 in.). In both series, each specimen had four mortar joints and five layers of 1.5 bricks. The samples were tested under monotonically increasing load applied along a diagonal. The average diagonal compression strength, computed by dividing the load at failure by the product of the length of the diagonal and the nominal thickness of the wall (92mm.), was 1.9 MPa -280 psi- (standard deviation = 0.28 MPa) for Series 1, and 1.8MPa -260 psi- (standard deviation = 0.4MPa) for Series 2.

4. TEST OF THE STRENGTHENED STRUCTURE

The fundamental period of the strengthened structure, estimated from free-vibration tests, was approximately 0.2sec. The strengthened structure was subjected to 20 displacement cycles. The maximum roof drift ratios reached in each cycle were: $\pm 0.025\%$, $\pm 0.05\%$, $\pm 0.15\%$, $\pm 0.25\%$, $\pm 0.50\%$, $\pm 0.75\%$, $\pm 1.00\%$, $\pm 1.25\%$, $\pm 1.50\%$, and $\pm 1.75\%$. Two cycles were applied at each target drift.

Gaps between columns and infill panels and cracks in the masonry were first observed at a drift ratio of 0.15%. The length of the gaps between the columns and the infill was measured to range between 1.5 and 2.0 m (60 and 80 in.). It is inferred that forces were transferred from columns to masonry and vice versa through a 92 mm (3-5/8-in.) wide and 0.75 to 1.3-m (30 to 50-in.) long area. The length of this area was observed to increase to 1.8-2.0 m (70-80 in.) as the drift ratio increased to 0.75%. Cracks in the masonry widened and additional cracks appeared as the drift ratio was increased, with the first perceptible and abrupt drop in stiffness caused by damage in walls at 0.2%. For a drift ratio of 0.25 %, the maximum crack width in the masonry was 4.0 mm (0.16 in.). Wider cracks were located in the first-story walls. At a drift ratio of 1.0%, cracks were visible in all three stories with a maximum crack width of 9.5 mm (3/8 in.).

Failure was judged to occur at a drift ratio of 1.75%. At this level of deformation, the walls in the third story showed perceptible distortion, second-story walls had large holes near mid-height and at lower corners, and first-story walls had holes in upper corners and the uppermost layer of brick had disintegrated. The crack patterns observed at the end of the second test are shown in Figure 3. The last displacement cycle completed before failure was done at a roof drift ratio of 1.5%. In this paper, this drift ratio is referred to as the displacement capacity of the strengthened structure.

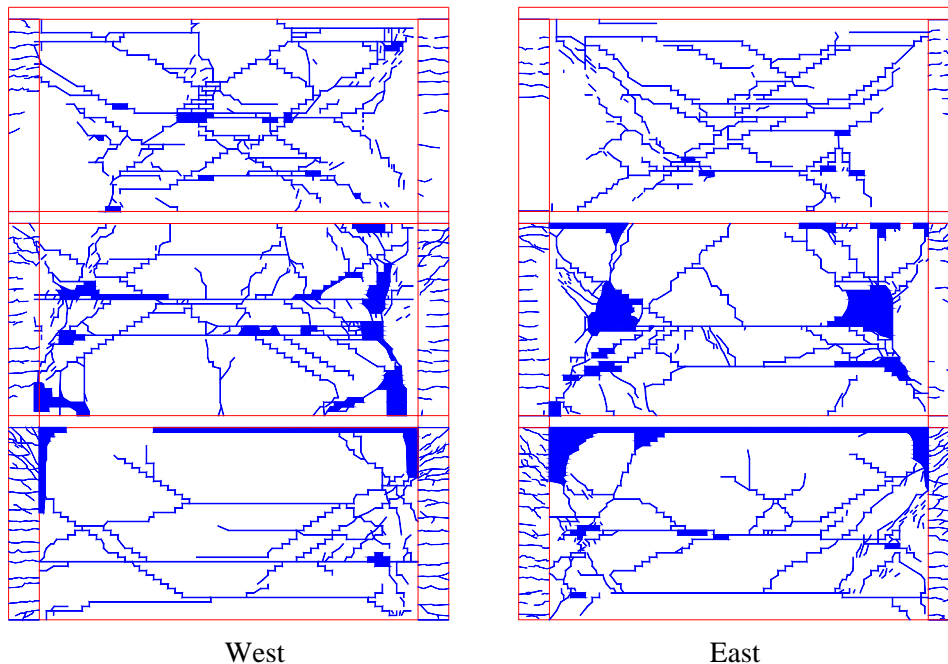
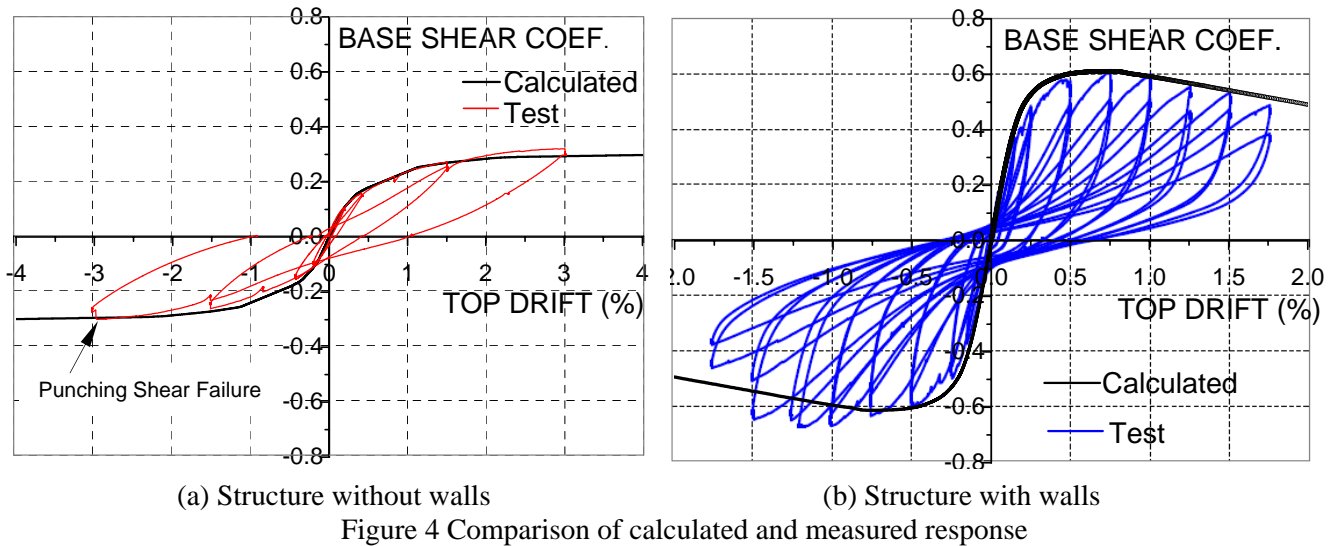


Figure 3. Crack Patterns Recorded after Completion of Tests.

Figure 4 shows the measured relationship between base shear coefficient (base shear divided by the structure weight including superimposed dead load) and roof drift ratio measured during the tests of the original and the strengthened structure. The data show that the addition of infill walls increased the initial stiffness of the structure by 500%, and the base shear coefficient by 100%.



5. NUMERICAL SIMULATIONS

Numerical simulations were carried out to estimate the probable response of the strengthened structure to eight earthquake records. The records considered are described in Table 1 in terms of magnitude, intensity, peak ground acceleration (PGA), peak ground velocity (PGV), distance to the epicenter, and soil conditions. The signals used as input in the numerical analyses were obtained by scaling the records in Table 1 to $PGV = 50 \text{ cm/s}$ (20 in/s). Other criteria to select records for dynamic analyses have been proposed by Rodriguez (2008). Relative displacement spectra computed for the scaled records and for linear oscillators with a damping factor of 0.02 are shown in Fig. 5.

Table 1. Selected Earthquake Records for Dynamic Analysis

Characteristics of Records (BEFORE scaling)									Response Measures (for SCALED records)	
Event	Record	Comp.	Soil	Ep. Dist (km)	Ms	MMI	PGA cm/s^2	PGV cm/s	V_E cm/s	V_D cm/s
California 18-V-1940	El Centro	N00W	Stiff	11	7.0	VII-VIII	341	38	93.2	72.9
Mexico 19-IX-1985	SCT	S00E	Clay	400	8.1	VIII-IX	98	38	10.5	5.2
Hyogoken-Nanbu 17-I-1995	Kobe JMA	N00E	Alluvium	10	6.9	VIII-IX	821	89	95.7	83.7
Northridge 17-I-1994	Sylmar Sta.M.	360°	Stiff	15	6.8	VIII-IX	827	129	61.9	52.0
Chile 3-III-1985	LLolleo	NE	Stiff	45	7.8	VIII	698	40	346	301.5
Miyagi 12-VII-1978	Tohoku	N00S	Alluvium	100	7.4	VII-VIII	258	37	82.6	66.9
Perú 15-VIII-2007	ICA University	NS	--	115	8.0 (Mw)	VII-VIII	334	64	58.1	36.7

The simulations consisted of nonlinear dynamic response analyses carried out using the program IDARC6.1. First, a numerical model was constructed and calibrated to represent the original test structure (without infill walls). The

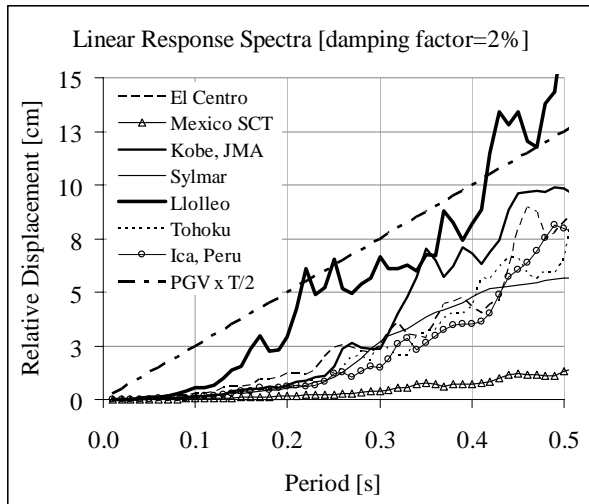


Figure 5 Linear Response Displacement Spectra (For Scaled Records)

slab was idealized by an equivalent beam of 3.0 m (10 ft) in width. The moment-curvature relationships for the equivalent beams and columns were calculated by the program using fiber models based on the measured material properties. Hysteretic response was idealized using the model proposed by Park et al. (1987). The parameters that control the shape of the hysteretic curves were set to HC=10, HBD=0.3, HBE=0.15, HS=1. The calculated relationship between roof drift and base shear coefficient is shown in Figure 4a. After this initial calibration, diagonal struts that represented the infill walls were added to the numerical model of the frame structure. The formulation proposed by Saneinejad and Hobbs (1995) was used to calculate the lateral strength and the lateral stiffness of the walls. The values calculated were 450 kN (100kip) and 80 kN/mm (460kip/in), respectively. In order to model the response of the infill walls, the program IDARC uses a smooth hysteretic model based on the Wen-Bouc model (Bouc, 1967; Baber and Noori, 1985). The parameters AIW, BTA, GMA and

ETA in Wen's model, parameters that govern the post yield ratio (ALPHIW), the slip (IS, AS, ZS, ZBS), the rate of stiffness decay (SK), the rate of strength decay (SP1, SP2) were set to the default values of IDARC (AIW=1.0; BTA=0.1; GMA=0.9; ETA=2.0; ALPHIW=0.01; IS=1; AS=0.3; ZS=0.1; ZBS=0.0; SK=0.1; SP1=0.8; SP2=1.0). The value of the parameter that controls the ductility capacity of the infill (MU) was set at MU=15.0 to fit the experimental results. Figure 4b shows the calculated lateral response obtained after calibration together with the experimental results.

After the numerical model of the building with walls was calibrated, dynamic analyses were performed. The results of these analyses are shown in Figure 6 and suggest that, for ground motions similar to those considered, the drift demand is not likely to exceed the drift capacity of the structure with infill walls (1.5%). The range of computed drift estimates is wide. Spectral ordinates (Fig. 5) and estimated energy input, E_I , varied drastically among the scaled records. The amounts of energy contributing to structural damage E_D , defined by Housner (1956) as $E_D = E_I - W_b$, were also different (Table 1). In this expression for E_D , W_b denotes the energy dissipated by damping, which was set to 5% of critical damping. In Table 1, both, E_I and E_D have been expressed in terms of equivalent velocities $V_E = \sqrt{2E_I / M}$ and $V_D = \sqrt{2E_D / M}$, where M is the total mass of the structure.

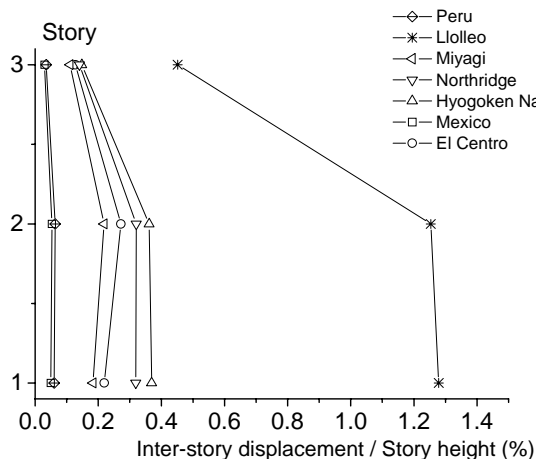


Figure 6 (a) Computed inter-story drift ratios

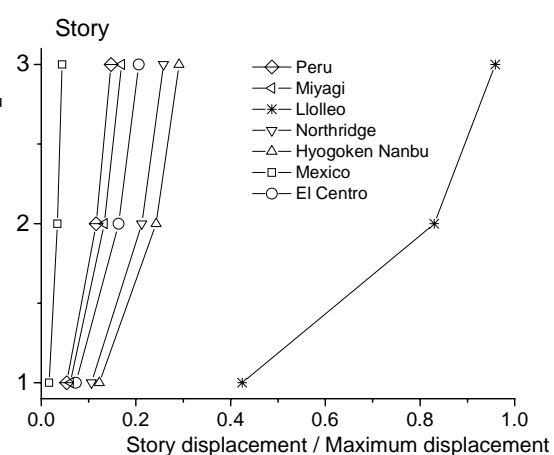


Figure 6 (b) Computed relative story displacement

The maximum inter-story drift ratio (DR_{max}) computed using nonlinear dynamic analyses matched an estimate obtained using the methodology proposed by Lepage (1997) which can be expressed as:

$$DR_{max} = \frac{\frac{1}{2} PGV \cdot \sqrt{2} \cdot T \cdot \Gamma \cdot \max(\phi_{i+1} - \phi_i)}{h_{story}} \quad (5.1)$$

PGV is peak ground velocity (50cm/s), T is initial period (0.2s), Γ is the participation factor for the first mode (inferred to be 1.25 from measurements of deflections caused by a linear distribution of loads), ϕ_i is the first-mode shape factor at level i (i=0,1,2,3), and h_{story} is story height. The factor $\max(\phi_{i+1} - \phi_i)$ was inferred to be approximately 2/5 from measurements of the deflected shape of the structure. With the parameters selected:

$$DR_{max} = \frac{\frac{1}{2} 50\text{cm/s} \cdot \sqrt{2} \cdot 0.2\text{s} \cdot 1.25 \cdot 0.4}{305\text{cm}} = 1.2\%$$

6. LIMITATIONS OF THE NUMERICAL MODEL

As shown in Figure 4, the calculated base shear-vs.-top drift response can be calibrated to match closely the envelope of the measured cyclic response of the building with and without infill walls. The analytical model, however, failed to produce a reasonable estimate of the displacement capacity of the structures tested.

The test of the strengthened structure was stopped when the maximum base shear reached in a cycle decreased to 2/3 of the maximum base shear reached in all previous cycles (Figure 4b). If the same criterion is used to define failure in the analyses, the computed drift ratio at “failure” is approximately 3.0%. This estimate of drift capacity is twice the measured drift capacity. Of course, the definition of a failure criterion would have been more difficult had there not been experimental results available.

7. CONCLUSIONS

A reinforced concrete structure was repaired and strengthened with solid brick infill walls. These walls were effective in increasing the strength (by 100%) and stiffness (by 500%) of the original reinforced concrete structure. The strengthened structure sustained drift reversals with amplitudes of up to 1.5% of the height of the structure without excessive stiffness reduction. Results from numerical simulations done using models calibrated to match test results suggest that it is very likely that the strengthened structure would not reach drift ratios exceeding 1.5% during ground motions similar to those considered (Table 1).

REFERENCES

- Bouc R. (1967). Forced Vibration of Mechanical Systems with Hysteresis. Proc. 4th Conference on Non-Linear Oscillations, Prague.
- Baber T.T. and Noori M. N. (1985). Random Vibration of Degrading Pinching Systems. *Journal of Engineering Mechanics*, **111**: 8, 1010-1026.

- Brokken, S.; Bertero, V.V. (1981). Studies on Effects of Infills in Seismic Resistant RC Construction. *Report UCB/EERC, 81-12, University of California, Berkeley, CA.*
- Calvi G. M., Bolognini, D. (2001). Seismic Response of Reinforced Concrete Frames Infilled with Masonry Panels Weakly Reinforced. *Journal of Earthquake Engineering* **5: 2**, 153-185.
- Crisafulli, F. J., Carr, A. J. and Park, R. (2000). Analytical Modeling of Infilled Frame Structures: A General Review. *Bull. of the New Zealand Society for Earthquake Engineering* **33:1**.
- Fick, D. (2008). Experimental Investigation of a Full-Scale Flat-Plate Reinforced Concrete Structure in the Inelastic Range of Response. Ph.D. Dissertation Thesis. Purdue University, W. Lafayette, IN.
- Fiorato, A. E., Sozen, M. A., Gamble, W. L. (1970). An Investigation of the Interaction of Reinforced Concrete Frames with Masonry Filler Walls. Civil Engineering Studies, University of Illinois, Urbana, IL, 525p.
- Hashemi, A., Mosalam, K. M. (2006). Shake-Table Experiment on Reinforced Concrete Structure Containing Masonry Infill Wall. *Earthquake Eng. Struct. Dyn.* **35: 14**, 1827–1852.
- Housner G. W (1956). Limit Design of Structures to Resist Earthquakes. Proc. 1st World Conference Earthquake Eng., Berkeley, California, 5-13.
- Lepage A. (1997) A Method for Drift-Control in Earthquake-Resistant Design of RC Building Structures. PhD Thesis, University of Illinois, Urbana, 251p.
- Matjaz D., Fajfar P. (2005). Simplified Non-linear Seismic Analysis of Infilled Reinforced Concrete Frames. *Earthquake Engineering and Structural Dynamics* **34:1**, 49–66.
- Negro P., Verzeletti, G. (1996). Effect of Infills on the Global Behaviour of Frames: Energy Considerations from Pseudodynamic Tests. *Earthquake Engineering and Structural Dynamics*, **25: 8**, 753-773
- Park Y. J, Reinhorn A. M. and Kunnath S. K. (1987). IDARC: Inelastic Damage Analysis of Reinforced Concrete Frame – Shear-Wall Structures. Technical Report NCEER-87-0008, State University of New York at Buffalo.
- Rodriguez M. E. (2008) Selecting Earthquake Records for Nonlinear Dynamic Analysis of Structures, Proc Seismic Engineering International Conference Commemorating the 1908 Messina and Reggio Calabria Earthquake.
- Saneinejad A. and Hobbs B. (1995). Inelastic Design of Infilled Frames. *Journal of Structural Engineering* **121: 4**, 634-650.
- Shimazaki K, Sozen M., Strong Ground Motion Drift and Base Shear Coefficient for RC Structures. Proc. 9th World Conference on Earthquake Eng., Tokyo and Kyoto, Japan, **5**, 165-170.
- Wood S. (1991). Performance of Reinforced Concrete Buildings During The 1985 Chile Earthquake : Implications for the Design of Structural Walls. *Earthquake Spectra*, **7:4**, 607-639.
- Zarnic R, Gosti S, Crewe AJ, Taylor CA (2001). Shaking Table Tests of 1:4 Reduced-Scale Models of Masonry Infilled Reinforced Concrete Frame Buildings. *Earthquake Engineering and Structural Dynamics* **30:6**, 819–834.